

JOINT INSTITUTE FOR NUCLEAR RESEARCH

Manuscript

UDK 539.172.128.17

PRONSKIKH

Vitaly Stanislavovich

INVESTIGATION OF PROTON-NUCLEAR REACTIONS

ON ISOTOPES ^{129}I , ^{237}Np AND ^{241}Am AT $E_p = 660$ MeV

Speciality: 01.04.16 –physics of atomic nuclei and elementary particles

Summary report of the thesis for the degree of
Philosophiae Doctor (Ph.D.) in Physics and Mathematics

Dubna 2005

Thesis is prepared at the V.I. Veksler – A.M. Baldin Laboratory of High Energies,
Joint Institute for Nuclear Research

Scientific supervisor (advisor): Doctor (Physics and Mathematics) Jindrich Adam

Official opponents:

Doctor of Science (Physics and Mathematics), Professor Titarenko Yury Efimovich
Doctor of Science (Physics and Mathematics), Professor Amelin Nikolai Sergeevich

Expert organization:

State Scientific Centre of the Russian Federation “A.I. Leipunsky Institute of
Physics and Power Engineering” (Obninsk, Russia).

Final presentation will take place at the meeting of the Dissertation Scientific
Council D 720.001.02 of Joint Institute for Nuclear Research on
“___”_____ 2005 at ___ pm at the address: Conference Hall of V.I.
Veksler – A.M. Baldin Laboratory of High Energies of Joint Institute for Nuclear
Research, 6, Joliot-Curie, Dubna, 141980 Russia.

Dissertation is available for examination at the Veksler — A.M. Baldin Laboratory
of High Energies of Joint Institute for Nuclear Research Scientific Library.

Summary of the Thesis was distributed on “___”_____ 2005.

Scientific Secretary of the Dissertation Scientific Council
Doctor of Science (Physics and Mathematics), Professor

Likhachev M.F.

General description: Investigations of the proton-nuclear reaction mechanisms at intermediate and high energies became very important in recent years due to a number of reasons. The reactions at low (<20 MeV) energies were studied during the last ten years in detail, and the data on these reactions have been published in the form of evaluated libraries. A large amount of data, both experimental and theoretical, in the region up to 200 MeV have recently been collected, while the data on reaction cross sections at energies higher than 200 MeV are incomplete and fragmentary. In this energy region changes in interaction mechanisms became evident, spallation, fission, and fragmentation reactions start to prevail, and the experimental methods of their investigation change accordingly. The number of open reaction channels becomes too large for creation of the evaluated libraries, and the calculation of necessary cross sections using theoretical computer models, which can then be incorporated in the codes for modelling of the industrial-scale systems, becomes more practical. Experimental investigation of proton-induced reactions, therefore, appears to be one of the basic methods for evolving of such theories.

Among contemporary and important areas of fundamental studies that require development of adequate nuclear reaction models are radioactive ion beams, astrophysics, and spallation neutron sources. Spallation neutron sources consist of an intense proton source and a heavy metal target. The fast neutrons, generated in spallation, are then moderated within heavy- or lightwater moderators. One of the very important applications of a spallation source is Accelerator Driven Transmutation System (hybrid reactor). In such systems spallation neutrons are used to sustain nuclear chain reaction in the subcritical reactor, whereas the long-lived reaction fragments can simultaneously transmute into the short-lived and stable isotopes in the subcritical blanket. Such system can produce electrical energy, part of which is spent to supply the accelerator work.

Accumulation of large amounts of long-lived radioactive isotopes is one of the most significant shortcomings of the present-day nuclear industry, which nevertheless remains an unavoidable mean of energy production within the next few decades. Radiation hazard assessments show that after isolation of the U-Pu series actinides, and such fission products as ^{99}Tc , ^{126}Sn , ^{90}Sr , ^{137}Cs , ^{129}I and ^{79}Se removal, ^{241}Am and ^{237}Np remain the key sources of the influence over the population. Among actinides, the largest contribution to the radioactivity is made by ^{241}Am , while ^{237}Np is predominant in the spent fuel in mass. Furthermore, ^{237}Np possesses a higher

mobility in biosphere in comparison with the other actinides, followed by higher probability of its penetration in body through food chains. Assessments reveal that after transmutation of all transuranic isotopes to stable, their total radioactivities would equalize in approximately 10^3 years, rather than in $5 \cdot 10^6$ years without such processing. Among the fission fragments, ^{129}I seems to be one of the most hazardous from biological standpoint.

Construction of subcritical reactor-transmuter is nowadays considered to be the most promising method for destruction of the components of spent nuclear fuel, and in this connection the need in data for the ADTS has grown significantly. Modelling of such systems requires experimental studying of interaction of high-energy particles with actinide and fission product nuclei, which can lead to advances in theoretical insights about these interactions and their computer models. Due to that experimental formation cross sections of the residual nuclides serve the differential parameter, comparison of which with calculations is optimal for the theoretical model development.

Aims of the study: This dissertation work is aimed at both experimental investigation of the residual nuclides formation at interactions of 660 MeV protons with ^{129}I , ^{237}Np and ^{241}Am isotopes using nuclear spectroscopy, and analysis of the measured cross sections using modern theoretical models. For solving of this task, the necessary spectroscopy methods were amended and developed, a program package was created.

Scientific novelty: The following new results were obtained in this research :

1. Techniques of the nuclide identification and short-lived β -unstable product formation cross section determination by means of activation analysis with HPGe γ -spectrometers have been amended using the precision nuclear spectroscopy approaches, a program package was created.
2. A technique was developed for calculation of optimal parameters of an experiment on studying individual product nuclei formed with small cross sections and situated in complex decay chains.
3. Experiments were carried out on determination of formation cross sections in reactions of protons of 660 MeV on the isotope ^{129}I . A total of 74 formation cross sections was determined for this target. These data were obtained for

the first time at intermediate energies.

4. Experiments were carried out on determination of formation cross sections in reactions of protons of 660 MeV on the isotope ^{237}Np . A total of 53 formation cross sections was determined for this target. These data were obtained for the first time at intermediate energies.
5. Experiments were carried out on determination of formation cross sections in reactions of protons of 660 MeV on the isotope ^{241}Am . A total of 80 formation cross sections was determined for this target. These data were obtained for the first time at high and intermediate energies.
6. An extensive analysis of the data using eleven modern existing theoretical models : LAHET (Bertini+RAL, ISABEL+RAL, INCL+RAL, INCL+ABLA), CASCADE, CEM95 (для ^{129}I), CEM2k (для ^{129}I), CEM2k+GEM2, LAQGSM+GEM2, CEM2k+GEMINI, LAQGSM+GEMINI was performed on the basis of both qualitative and quantitative criteria, which showed insufficient for practical purposes precision of modelling of the reactions under study.

Practical value: Results presented in the dissertation can be used in the following way:

1. Cross section determination methods for the short-lived nuclear reaction products can be used in activation analysis and radiation medicine, they are used for reaction rate determination in activation detectors and transmutation samples.
2. Optimal experimental parameter calculation methods are used for planning, carrying out, and data analysis of the experiments on investigation of product nuclei, formed with small cross sections and positioned in complex decay schemes.
3. Cross sections of the proton-induced reactions in ^{129}I , ^{237}Np and ^{241}Am targets and the results of their analysis with theoretical models are necessary for investigations of these reactions' mechanisms as well as in applied research for development of ADS modelling tools.
4. Obtained experimental results can be used for filling the nuclear data libraries (EXFOR, NSR).

Approbation of the Thesis: The dissertation is based on the works [1-8] reported at the seminars of the Dzhelapov Laboratory of Nuclear Problems of Joint Institute for Nuclear Research, scientific conferences of the Association of Young Scientists and Specialists of JINR /Dubna (1999, 2002)/, International Conferences on Nuclear Spectroscopy and Structure of Atomic Nucleus /Obninsk (1997), Moscow (1998), Saint-Petersburg (2000), Sarov (2001), Moscow (2003)/, Conference of the US Radiochemical Society /San-Diego (2001)/, Workshop on Nuclear Reaction Data and Nuclear Reactors at International Centre for Theoretical Physics, Italy /Trieste (2002)/, International Conferences on Nuclear for the Transmutation on Nuclear Waste, Germany /Darmstadt (2003)/, Specialists' Meeting Shielding Aspects of Accelerators, Targets and Irradiated Facilities SATIF-7, Portugal /Sacavem (2004)/, International Conferences on Nuclear Data for Science and Technology, Japan /Tsukuba (2002)/, USA /Santa Fe, NM (2004)/.

Structure of the Thesis: The dissertation consists of an introduction, three chapters, conclusion, acknowledgements, and a list of references. The overall text size including 35 figures, 17 tables and a list of references containing 99 items amounts to 131 pages. The main results of the dissertation have been published in 8 co-authored papers (67 pages of published text). The principal contribution to these works was made by the author of this Thesis.

Contents of the Thesis: in **Introduction** the topicality of studies of proton-induced reactions at high and intermediate energies is discussed, a qualitative description of the processes of interaction of intermediate energy protons with nuclei and a survey of the theoretical models employed is given, the aim of the study is formulated and a short summary of the dissertation is presented.

First Chapter is devoted to the discussion of the problems and methods of analysis of γ -spectra measured with semiconductor detectors. In investigations of nuclear structure as well as residual nuclei formation cross sections a number of tasks arise, some of which were solved in this work. Among them are developing of the method for optimal experimental parameter calculation, precise determination of half-lives from short-lived nuclei decays measured with semiconductor detectors, application of the precision spectroscopy approaches in activation measurements, and automation of γ -spectra analysis. The γ -spectra are measured in the energy range from 50 to 3500 keV with the use of the spectrometers with HPGe-detectors. In the course of the data analysis, the radioactive background as well as the target spectrum before

irradiation were taken into consideration. In separate measurements intensities of single and double escape peaks, which moderately depend on particular measurement geometry. An analytical curve in of the form : $I_{\gamma}^{esc}/I_{\gamma} = \sum_{i=1}^4 a_i(\ln(E_{\gamma}))^i$, fitted to the ratios of the escape peak intensities to the respective photopeaks was used for correcting the γ -line areas in the spectra. An 8-th degree function of the same form was also used to describe the photopeak registration efficiency of the HPGe-detector. In the course of the residual nuclide identification, their $T_{1/2}$ as well as their γ -transition energies and relative intensities were taken into account, which appeared to be especially important when analyzing complex peaks. A criterion $K = (I_{\gamma}^{lit} \cdot I_{\gamma,max}^{exp}) / (I_{\gamma}^{exp} \cdot I_{\gamma,max}^{lit})$ was used, where I_{γ}^{lit} and $I_{\gamma,max}^{lit}$ are adopted intensities of the transition under analysis and the reference transition, while I_{γ}^{exp} and $I_{\gamma,max}^{exp}$ are their experimental intensities. In case of correct identification and absence of peak overlaps, this criterion is to be equal to unity in the range of two uncertainties; if a peak of an isotope is absent in the spectrum, $K < 1$ for the upper limit of its detection.

As the spectra investigated are very complex and the γ -line overlap probability for different isotopes is very high, in the case of an admixture detection such lines were decomposed into components using the least squares method. Different possibilities of genetic relations between the isotopes found were considered. For the purpose of precision spectra analysis¹, spurious, background and escape peak subtraction, their identification, decomposition and cross section calculations a package of PC programs has been created [1].

One of the most important parameters influencing reliability of radioactive nucleus identification is its half-live $T_{1/2}$. Employing modern types of electronics units in spectrometers requires refinement of $T_{1/2}$ measurement methods, and thorough assessment of properties of each configuration. Basically, when a short-lived radioactive source is measured during the time comparable with its $T_{1/2}$, deadtime of the spectrometer changes almost proportionally to its activity, and the equation for its γ -peak area in spectra has the form :

$$S_i \frac{\Delta t_i^r}{\Delta t_i^l} = N_0 \{ (e^{-\lambda t_i} - e^{-\lambda(t_i + \Delta t_i^r)}) + C_1 (e^{-2\lambda t_i} - e^{-2\lambda(t_i + \Delta t_i^r)}) + C_2 (e^{-3\lambda t_i} - e^{-3\lambda(t_i + \Delta t_i^r)}) \}, \quad (1)$$

¹Preliminary data processing was performed with the program `deimos32` from NPI, Řež

N_0 – initial number of nuclei, t_i – measurement start time, Δt_i^r и Δt_i^l – real and live times of measurement.

When analyzing spectra of a β^- -decaying nuclide ^{140}La , formed in the reaction $^{139}\text{La}(n, \gamma)^{140}\text{La}$, measured using a γ -spectrometer assembled of a HPGe 28%-efficiency detector ORTEC, a spectroscopy amplifier CANBERRA 2026, and a multi-channel analyzer SPECTRUM MASTER 919 with an automatic deadtime determination, it appeared that the deadtime found in a conventional way (using only the first term of the equation (1)) differs from the one recommended by Nuclear Data Sheets by 12σ , whereas the maximum deadtime of the setup amounted to 8%. Additional experiments were carried out, in which ^{139}La samples were irradiated in a thermal neutron flux of the microtron MT-25, deadtimes varying from 1 to 50%. It was shown [2] that at a 50% deadtime, its underestimation by the setup leads to depreciation of γ -line areas by 10%, while the correct $T_{1/2}$ value is attained only by using of all the three terms in (1). These experiments allowed to clarify the reasons of observed differences of ^{140}La half-lives determined in a series of activation measurements with large loads from the adopted value, and correspond them to systematic uncertainties arising from neglecting the second and third terms in (1), as well as to determine the value of $T_{1/2}(^{140}\text{La}) = \mathbf{1.6808 (18) \text{ days}}$ [2].

In experiments with spallation products it often appears that the product nuclei formed find themselves in complex decay chains, and several targets of the same isotope are irradiated and measured several times, irradiation time t_1 , delay time t_2 and measurement time t_3 varying in a broad range. In this connection two problems were solved in this work : to determine formation cross sections of daughter nuclei in

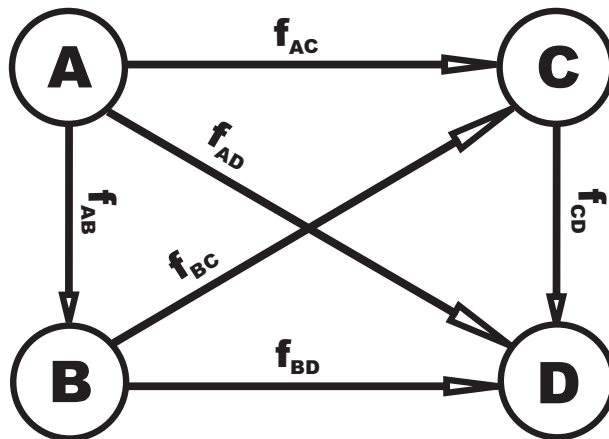


Figure 1: General view of decay scheme of four nuclei (or their excited states).

a complex chain, and to find optimum t_1 , t_2 and t_3 for accumulation of desired nuclide situated in such a chain. For the practical purpose it is enough to confine ourself to a chain of four nuclei (see **Figure 1**), which limitation is required by

finite statistics in γ -spectra. The number of genetically related nuclei $N_A(t)$, $N_B(t)$, $N_C(t)$ and $N_D(t)$ during the irradiation, delay, or measurement is described by the simultaneous differential equations :

$$\begin{cases} dN_A(t)/dt = Q_A - \lambda_A N_A(t) \\ dN_B(t)/dt = Q_B - \lambda_B N_B(t) + f_{AB} \lambda_A N_A(t) \\ dN_C(t)/dt = Q_C - \lambda_C N_C(t) + f_{AC} \lambda_A N_A(t) + f_{BC} \lambda_B N_B(t) \\ dN_D(t)/dt = Q_D - \lambda_D N_D(t) + f_{AD} \lambda_A N_A(t) + f_{BD} \lambda_B N_B(t) + f_{CD} \lambda_C N_C(t), \end{cases}$$

where Q is formation rate of a given isotope (during delay and measurement $Q = 0$). Such sets were solved for each of the t_1 , t_2 and t_3 intervals (see **Figure 2**), while their solution appeared to be convenient to find in the form of recurrence relations. Thus, for estimation of independent formation cross sections, the following set of linear equations is solved by the least squares method :

$$\begin{cases} S_\gamma^i \frac{\Delta t_3^{r,i}}{\Delta t_3^{l,i}} K_{x_A} = A_A^i \sigma_A, \\ S_\gamma^i \frac{\Delta t_3^{r,i}}{\Delta t_3^{l,i}} K_{x_B} = A_B^i \sigma_A + B_B^i \sigma_B, \\ S_\gamma^i \frac{\Delta t_3^{r,i}}{\Delta t_3^{l,i}} K_{x_C} = A_C^i \sigma_A + B_C^i \sigma_B + C_C^i \sigma_C, \\ S_\gamma^i \frac{\Delta t_3^{r,i}}{\Delta t_3^{l,i}} K_{x_D} = A_D^i \sigma_A + B_D^i \sigma_B + C_D^i \sigma_C + D_D^i \sigma_D, \end{cases}$$

where S_γ^i is the peak area with E_γ in i -th measurement, K_{x_j} is a function depending on the γ -detector efficiency, γ -quanta intensity, number of target nuclei, and number of protons, A_j , B_j , C_j and D_j are some recurring equations deduced. Analogous formulae were obtained also for cumulative cross sections. All the recurring coefficients are presented in [3] in detail.

As the main criterion of success in an experiment is the measurement of an effect (peak area) with the least possible uncertainty, the peak area N , referring to decay of j -th nuclei (for instance, of sort B), is proportional to the number of nuclei of this sort $\mathfrak{R}_j(t_3)$, decayed during the measurement time, $N = k\mathfrak{R}_j(t_3)$, where the forms of \mathfrak{R}_j for various nuclei of the chain are deduced in [3]. The other nuclei (A , C , D) produce a spurious background $\mathfrak{R}_f(t_3) = \mathfrak{R}_A(t_3) + \mathfrak{R}_C(t_3) + \mathfrak{R}_D(t_3)$, thus the number of collected background events $\Phi = k\mathfrak{R}_f(t_3)$, and the total number of events $T = N + \Phi$.

On assumption of cyclic measurement regime, for the number of cycles one can write : $c = \Delta t_T / (\Delta t_1 + \Delta t_2 + \Delta t_3)$. Taking into account that the decays of j and f nuclei are statistically independent, and the uncertainties of numbers of collected events are added in the following way : $\Delta_N^2 = \Delta_T^2 + \Delta_\Phi^2$, and the relative measurement error equals to $\Delta N/N$, the following quality criterion of an experiment (figure of merit) was obtained :

$$K_e = \frac{\mathfrak{R}_j(t_3)}{\sqrt{\mathfrak{R}_j(t_3) + 2\mathfrak{R}_f(t_3)}} \sqrt{ck}.$$

As at the planning stage of an experiment k and t_T are often to be defined in advance, a provision made in the program `optimum`, created in this work, to vary each of the parameters t_1 , t_2 and t_3 with a predefined step, finding maxima of the objective function K_e . The calculations performed for the isobar with $A = 152$ were published in [3]. The approach is proposed to use for selection of optimal conditions for measurements of spallation products, especially those formed with small cross sections, and if the problem to solve is to study individual isotopes. This method will give the best results in the case of using, for example, a device for transporting products to detectors.

In the **Chapter Two** experiments on determination of proton-induced reaction cross sections on isotopes ^{129}I , ^{237}Np and ^{241}Am at the proton energy 660 MeV are described. The experiments were carried out at the extracted proton beam of Phasotron with the beam current 1.2 mA. The targets consisted of NpO_2 , AmO_2 and NaI (15% ^{127}I + 85% ^{129}I). The samples were weld-sealed in aluminium containers, 79 g in weight. (see **Figure 3**). Characteristics of the targets and beam are presented in **Table 1**. Two targets of each nuclide were irradiated in all. The beam size and position were checked by a two-coordinate proportional chamber. For the purpose of monitoring, reaction $^{27}\text{Al}(p, 3pn)^{24}\text{Na}$ was employed, and Al foils of the same size as the target nuclide spots and 99 mg in weight were used as monitors.

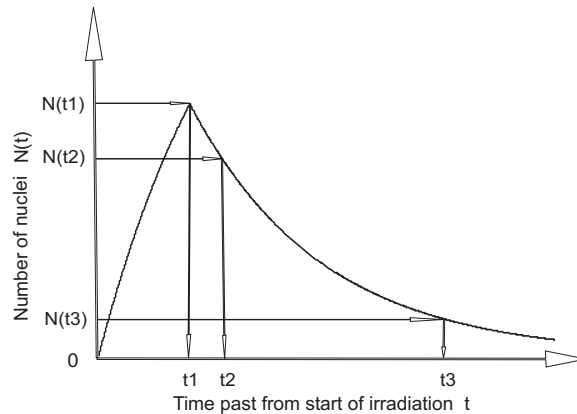


Figure 2: Nuclei accumulation diagram in a decay chain.

Table 1: Characteristics of the ^{237}Np , ^{241}Am and ^{129}I targets and the proton beam.

Target nuclide	$^{237}\text{Np}_{93}$		$^{241}\text{Am}_{95}$		$^{129}\text{I}_{53}$	
Half-live, y	2.144(7) 10^6		432.2(7)		15.7(4) 10^6	
Target weight, g	0.742	0.742	0.177	0.183	0.500	0.500
Target thickness, mm	0.193	0.193	0.043	0.044	0.395	0.395
Initial activity, mCi	0.523	0.523	601	621	0.063	0.063
Beam intensity, 10^{14} p/min	2.64	2.66	2.72	2.58	2.68	2.68
Irradiation time, min	5	30	5	30	5	30

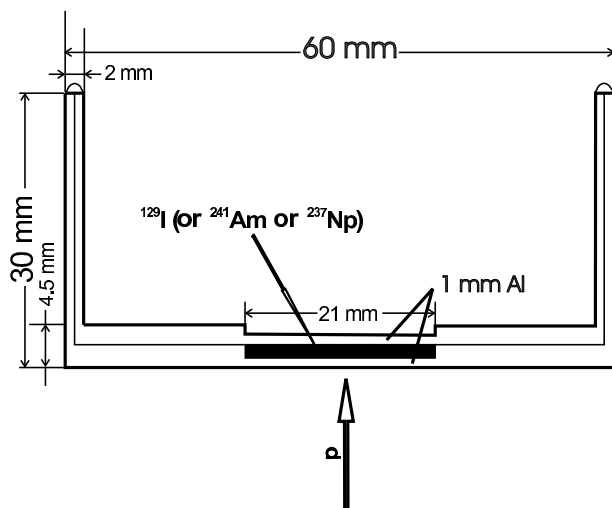


Figure 3: Weld sealed aluminium containers with radioactive samples used, prepared in IPPE, Obninsk.

spectra was carried out with the help of MASTER 921 (^{241}Am and ^{129}I) and MASTER 919 (^{237}Np) analyzers, which automatically determined deadtime of the spectrometer.

Counting of the first set of targets was started 10 minutes after the end of their irradiation, 17 spectra were taken from each sample, measurement time ranging from 5 minutes to 3 hours, initial distances from samples to respective detectors made 225 cm for ^{129}I , 150 cm for ^{241}Am and 100 cm for ^{237}Np . Measurement of the second set of ^{129}I samples (30-minute exposures) was started 20 hours after the end of irradiation (17 hours for ^{241}Am and ^{237}Np), 13 spectra were taken during 33 days

For reducing of the targets' own background, a shielding of a 10 mm thick Pb, 2 mm thick Cd, and 1 mm thick Cu plates was mounted on the detector. Activity induced in the targets was counted with the help of three semiconductor γ -detectors : 1) the ^{129}I target at a HPGe detector with efficiency $\varepsilon_\gamma = 50\%$ and energy resolution $E_\gamma = 2.15$ keV at the line 1332 keV (^{60}Co); 2) the ^{241}Am target at a HPGe detector with $\varepsilon_\gamma = 20\%$ and $E_\gamma = 1.8$ keV; 3) the ^{237}Np at a Ge(Li) detector with $\varepsilon_\gamma = 4.8\%$ and $E_\gamma = 2.6$ keV. Acquiring of γ -

(11 during 30 days for ^{241}Am and ^{237}Np), counting time varied from 5 to 66 hours (50 hours for ^{241}Am and ^{237}Np). Using the developed program package [2], energies and intensities of γ -transitions in the residual nuclei were determined, as well as the peak registration limits on a given background. With the use of the programs, background, single and double escape peaks were found, and if their overlaps with the photopeaks were detected, intensities of the latter were corrected. Using corrected γ -lines, half-lives of isotopes were determined where possible. Residuals were then identified using energies of their γ -lines, half-lives, and if several γ -lines of the same nucleus were found, also ratios of their intensities, which was compared with that from recommended data sets. In total, more than 2800 γ -lines in the spectra of ^{129}I target, more than 1000 in the spectra of ^{241}Am , and more than 500 in the spectra of ^{237}Np were found, formation cross sections of 74 product nuclei in ^{129}I , 80 – in ^{241}Am and 53 – in ^{237}Np targets were determined. Final experimental results for all the three targets are presented in **Tables 2-4**. In the **Tables**, cumulative cross sections are denoted by the letter “C”, independent – “I”, isomer transition – “IT”, β^+ , β^- – beta-decay, ε – electron capture.

Table 2: Experimental data for the target $^{129}\text{I}+^{127}\text{I}$.

Isotope	$T_{1/2}$	Decay mode	σ_{exp} , mb	Isotope	$T_{1/2}$	Decay mode	σ_{exp} , mb
^{44m}Sc	2.44 d	I(IT, ε)	0.20(4)	^{104}Ag	69.2 m	I(ε , β^+)	8.3(8)
^{46}Sc	83.83 d	C(β^-)	0.36(4)	^{105}Ag	41.29 d	C(ε)	14.3(17)
^{48}V	15.97 d	C(β^+ , ε)	0.58(6)	^{106}Ag	8.46 d	I(ε)	7.5(7)
^{52}Mn	5.29 d	C(ε , β^+)	0.37(5)	^{108}In	58 m	I(β^+ , ε)	7.1(7)
^{56}Co	78.8 d	C(ε , β^+)	0.11(4)	^{109}In	4.20 h	I(ε , β^+)	12.1(12)
^{58}Co	70.92 d	C(ε , β^+)	0.47(15)	^{109}Sn	18.0 m	C(ε , β^+)	3.02(30)
^{59}Fe	44.5 d	C(β^-)	0.065(7)	^{110m}Ag	249.9 d	I(β^- ,IT)	1.50(18)
^{65}Zn	244.1 d	C(ε , β^+)	0.88(9)	^{110}In	4.9 h	I(ε)	11.7(12)
^{72}As	26 h	I(β^+ , ε)	0.93(9)	^{110m}In	69.1 m	C(ε)	6.4(8)
^{72}Se	8.4 d	C(ε)	0.59(15)	^{113}Sn	115.1 d	C(ε)	27.2(30)
^{74}As	17.78 d	I(ε , $\beta^{+/-}$)	0.85(9)	^{114m}In	49.51 d	I(IT, ε)	7.1(7)
^{76}Br	16.2 h	C(β^+ , ε)	0.77(9)	^{114}Sb	3.49 m	C(ε , β^+)	2.92(35)
^{77}Br	2.38 d	C(ε , β^+)	0.64(15)	^{115m}In	4.49 d	I(IT, β^-)	15.6(35)
^{83}Rb	86.2 d	C(ε)	0.40(8)	^{115}Sb	32.1 m	C(ε , β^+)	20.0(30)
^{84}Rb	32.87 d	I(ε , $\beta^{+/-}$)	0.12(4)	^{116m}In	54.15 m	I(β^-)	2.72(42)

Table 2: Experimental data for the target $^{129}\text{I}+^{127}\text{I}$ (continued).

Isotope	$T_{1/2}$	Decay mode	σ_{exp} , mb	Isotope	$T_{1/2}$	Decay mode	σ_{exp} , mb
^{85}Sr	64.84 d	$\text{C}(\varepsilon)$	1.49(16)	^{116}Sb	15.8 m	$\text{I}(\beta^+, \varepsilon)$	2.0(4)
^{86}Y	14.74 h	$\text{C}(\beta^+, \varepsilon)$	0.69(25)	^{116m}Sb	60.3 m	$\text{I}(\varepsilon, \beta^+)$	11.6(14)
^{87}Y	3.35 d	$\text{C}(\varepsilon, \beta^+)$	1.15(11)	^{116}Te	2.49 h	$\text{C}(\varepsilon, \beta^+)$	9.9(10)
^{88}Y	106.6 d	$\text{I}(\varepsilon, \beta^+)$	0.36(10)	^{117}In	43.8 m	$\text{I}(\beta^-)$	1.6(3)
^{88}Zr	83.4 d	$\text{C}(\varepsilon)$	1.4(4)	^{117}Te	1.03 h	$\text{C}(\varepsilon, \beta^+)$	15.4(15)
^{89}Zr	3.27 d	$\text{C}(\varepsilon, \beta^+)$	1.51(15)	^{118m}Sb	5.00 h	$\text{I}(\varepsilon, \beta^+)$	11.1(12)
^{90}Nb	14.60 h	$\text{C}(\beta^+, \varepsilon)$	1.18(13)	^{118}Te	6.00 d	$\text{I}(\varepsilon)$	13.9(14)
^{92m}Nb	10.15 d	$\text{I}(\varepsilon, \beta^+)$	0.11(4)	^{118}I	13.7 m	$\text{C}(\beta^+, \varepsilon)$	3.3(4)
^{93m}Mo	6.85 h	$\text{I}(\text{IT}, \varepsilon)$	0.94(30)	^{119}Te	16.05 h	$\text{C}(\varepsilon, \beta^+)$	11.5(12)
^{93}Tc	2.75 h	$\text{C}(\varepsilon, \beta^+)$	2.14(24)	^{119m}Te	4.69 d	$\text{I}(\varepsilon, \beta^+)$	16.1(15)
^{94}Tc	4.88 h	$\text{I}(\varepsilon, \beta^+)$	1.79(17)	^{120m}Sb	5.76 d	$\text{I}(\varepsilon)$	6.3(6)
^{94m}Tc	52 m	$\text{I}(\beta^+, \varepsilon)$	0.44(8)	^{120}I	1.35 h	$\text{C}(\beta^+, \varepsilon)$	10.2(12)
^{95}Nb	34.98 d	$\text{C}(\beta^-)$	0.36(5)	^{120m}I	53.0 m	$\text{I}(\beta^+, \varepsilon)$	2.9(3)
^{95}Tc	20.0 h	$\text{C}(\varepsilon)$	3.00(34)	^{121}Te	16.8 d	$\text{C}(\varepsilon)$	17.9(18)
^{96}Tc	4.28 d	$\text{I}(\varepsilon)$	2.50(25)	^{121m}Te	154.0 d	$\text{I}(\text{IT}, \varepsilon)$	13.3(16)
^{99}Rh	16.0 d	$\text{I}(\varepsilon, \beta^+)$	0.84(25)	^{122}Sb	2.70 d	$\text{C}(\varepsilon, \beta^{+/-})$	7.7(9)
^{100}Rh	20.8 h	$\text{I}(\varepsilon, \beta^+)$	4.21(50)	^{123}I	13.2 h	$\text{C}(\varepsilon)$	25.0(24)
^{100}Pd	3.63 d	$\text{C}(\varepsilon)$	2.85(33)	^{124}I	4.18 d	$\text{I}(\varepsilon, \beta^+)$	26.3(30)
^{101m}Rh	4.34 d	$\text{I}(\varepsilon, \beta^+)$	2.9(9)	^{126}Sb	12.4 d	$\text{I}(\beta^-)$	0.54(5)
^{101}Pd	8.47 h	$\text{C}(\varepsilon, \beta^+)$	6.3(8)	^{126}I	13.02 d	$\text{I}(\text{IT})$	35(5)
^{102}Rh	2.9 Y	$\text{I}(\varepsilon)$	2.98(30)	^{127}Xe	36.46 d	$\text{C}(\varepsilon)$	3.8(4)
^{103}Ru	39.25 d	$\text{C}(\beta^-)$	0.43(5)	^{128}I	25.0 m	$\text{I}(\beta^-, \varepsilon)$	31(5)

Table 3: Experimental data for the target ^{237}Np .

Isotope	$T_{1/2}$	Decay mode	σ_{exp} , mb	Isotope	$T_{1/2}$	Decay mode	σ_{exp} , mb
^{48}Sc	1.82 d	$\text{I}(\beta^-)$	5.2(15)	^{122}Sb	2.7 d	$\text{C}(\beta^-)$	19(4)
^{48}V	15.97 d	$\text{C}(\beta^+)$	0.89(20)	^{124}Sb	60.2 d	$\text{C}(\beta^-)$	16.7(20)
^{56}Mn	2.58 h	$\text{C}(\beta^-)$	25.4(45)	^{126}Sb	12.4 d	$\text{C}(\beta^-)$	13.9(20)
^{74}As	17.77 d	$\text{I}(\beta^-, \varepsilon)$	3.6(5)	^{127}Sb	3.85 d	$\text{C}(\beta^-)$	14.7(20)

Table 3: Experimental data for the target ^{237}Np (continued).

Isotope	$T_{1/2}$	Decay mode	σ_{exp} , mb	Isotope	$T_{1/2}$	Decay mode	σ_{exp} , mb
^{83}Rb	86.2 d	$\text{C}(\epsilon)$	6.1(8)	^{128}Sb	9.01 h	$\text{C}(\beta^-)$	90(10)
^{84}Rb	32.77 d	$\text{C}(\beta^+, \beta^-)$	13.3(16)	^{132}Te	3.26 d	$\text{C}(\beta^-)$	13(3)
^{86}Rb	18.63 d	$\text{C}(\beta^-)$	17.7(20)	^{133m}Te	55.4 m	$\text{I}(\beta^+, \text{IT})$	18(4)
^{85}Sr	64.84 d	$\text{C}(\epsilon)$	9.6(20)	^{124}I	4.18 d	$\text{I}(\beta^+, \epsilon)$	17.3(20)
^{91}Sr	9.63 h	$\text{C}(\beta^-)$	29(3)	^{131}I	8.04 d	$\text{C}(\beta^-)$	20(4)
^{87}Y	3.35 d	$\text{C}(\beta^+, \epsilon)$	6.7(8)	^{134}I	52.5 m	$\text{C}(\beta^-)$	12.9(15)
^{88}Y	106.6 d	$\text{C}(\beta^+, \epsilon)$	10.4(19)	^{136}Cs	13.16 d	$\text{C}(\beta^-)$	9.1(13)
^{89}Zr	3.27 d	$\text{C}(\epsilon)$	4.6(5)	^{138}Cs	33.41 m	$\text{C}(\beta^-)$	14.9(29)
^{95}Zr	64.02 d	$\text{C}(\beta^-)$	59(6)	^{131}Ba	11.5 d	$\text{C}(\beta^+, \epsilon)$	71(13)
^{95}Nb	33.15 d	$\text{C}(\beta^-)$	22(4)	^{140}Ba	12.75 d	$\text{C}(\beta^-)$	23(4)
^{99}Mo	2.75 d	$\text{C}(\beta^-)$	73(13)	^{145}Eu	5.93 d	$\text{C}(\beta^+, \epsilon)$	0.83(9)
^{95m}Tc	61 d	$\text{C}(\beta^+, \epsilon)$	2.3(4)	^{146}Eu	4.59 d	$\text{I}(\beta^+, \epsilon)$	4.2(6)
^{96}Tc	4.98 d	$\text{C}(\beta^+, \epsilon)$	5.7(9)	^{147}Eu	24.1 d	$\text{C}(\beta^+, \epsilon)$	1.9(6)
^{103}Ru	39.26 d	$\text{C}(\beta^-)$	63(7)	^{146}Gd	48.27 d	$\text{C}(\epsilon)$	1.39(16)
^{105}Ru	4.44 h	$\text{C}(\beta^-)$	19.6(20)	^{152}Tb	17.5 h	$\text{C}(\beta^+, \epsilon)$	27(3)
^{106m}Rh	2.17 h	$\text{I}(\beta^-)$	55(9)	^{171}Lu	8.24 d	$\text{C}(\beta^+, \epsilon)$	2.4(10)
^{106m}Ag	8.28 d	$\text{I}(\beta^+, \epsilon)$	6.2(8)	^{185}Os	93.6 d	$\text{C}(\epsilon)$	2.8(4)
^{110m}Ag	249.49 d	$\text{I}(\beta^-, \epsilon)$	18.0(20)	^{188}Pt	10.2 d	$\text{C}(\epsilon)$	0.46(8)
^{115}Cd	2.23 d	$\text{C}(\beta^-)$	65(12)	^{206}Po	8.8 d	$\text{C}(\beta^+, \epsilon)$	3.8(7)
^{117m}Cd	3.46 h	$\text{C}(\beta^-)$	17(4)	^{230}Pa	17.4 d	$\text{I}(\beta^+, \epsilon)$	1.6(3)
^{125}Sn	9.64 d	$\text{C}(\beta^-)$	6.6(11)	^{234}Np	4.4 d	$\text{C}(\beta^+, \epsilon)$	2.2(4)
^{118m}Sb	5 h	$\text{I}(\beta^+, \epsilon)$	10.4(13)	^{238}Np	2.12 d	$\text{I}(\beta^-)$	16(3)
^{120m}Sb	5.76 d	$\text{I}(\beta^+, \epsilon)$	14.7(16)				

Table 4: Experimental data for the target ^{241}Am .

Isotope	$T_{1/2}$	Decay mode	σ_{exp} , mb	Isotope	$T_{1/2}$	Decay mode	σ_{exp} , mb
^{48}Sc	1.82 d	$\text{I}(\beta^-)$	1.11(20)	^{108m}Rh	6 m	$\text{I}(\beta^-)$	11.6(15)
^{48}V	15.97 h	$\text{C}(\beta^+)$	3.4(5)	^{112}Pd	21.01 h	$\text{C}(\beta^-)$	21.0(28)
^{52}V	3.74 m	$\text{C}(\beta^-)$	2.3(6)	^{106m}Ag	8.28 d	$\text{I}(\beta^{+/-})$	2.5(3)

Table 4: Experimental data for the target ^{241}Am (continued).

Isotope	$T_{1/2}$	Decay mode	σ_{exp} , mb	Isotope	$T_{1/2}$	Decay mode	σ_{exp} , mb
^{52}Mn	5.59 d	$\text{C}(\beta^+, \epsilon)$	1.74(28)	^{110m}Ag	249.49 d	$\text{I}(\beta^-, \epsilon)$	11.6(24)
^{54}Mn	312.3 d	$\text{I}(\epsilon)$	10.1(14)	^{112}Ag	3.130 h	$\text{I}(\beta^-)$	20(4)
^{56}Mn	2.58 h	$\text{C}(\beta^-)$	6.7(16)	^{115}Cd	2.23 d	$\text{C}(\beta^-)$	19.2(28)
^{72}Ga	14.1 h	$\text{C}(\beta^-)$	1.5(7)	^{117m}Cd	3.46 h	$\text{C}(\beta^-)$	6.9(7)
^{72}As	26 h	$\text{C}(\beta^+, \epsilon)$	4.2(5)	^{116m}In	54.41 m	$\text{I}(\beta^-)$	16.4(24)
^{76}As	1.08 d	$\text{I}(\beta^+)$	4.5(16)	^{117m}In	116.2 m	$\text{C}(\beta^-)$	21(3)
^{76}Br	16.2 h	$\text{C}(\beta^+)$	0.6(18)	^{118m}In	4.45 m	$\text{I}(\beta^-)$	6.5(9)
^{82}Br	35.3 h	$\text{I}(\beta^-)$	8.0(11)	^{118m}Sb	5 h	$\text{I}(\beta^+, \epsilon)$	7.6(14)
^{84m}Br	6 m	$\text{C}(\beta^-)$	2.7(6)	^{120}Sb	15.89 m	$\text{I}(\beta^+, \epsilon)$	10.8(14)
^{84}Br	31.8 m	$\text{I}(\beta^-)$	9.2(14)	^{122}Sb	2.7 d	$\text{C}(\beta^-, \epsilon)$	14.0(19)
^{82m}Rb	6.47 h	$\text{C}(\beta^+, \epsilon)$	2.1(10)	^{124}Sb	60.2 d	$\text{C}(\beta^-)$	10.2(14)
^{84m}Rb	32.77 d	$\text{C}(\beta^+/-)$	6.9(11)	^{126}Sb	12.46 d	$\text{C}(\beta^-)$	7.3(14)
^{86}Rb	18.63 d	$\text{C}(\beta^-)$	2.02(29)	^{127}Sb	3.85 d	$\text{C}(\beta^-)$	7.3(12)
^{89}Rb	15.15 m	$\text{C}(\beta^-)$	11.1(15)	^{128}Sb	9.01 h	$\text{C}(\beta^-)$	3.3(10)
^{91}Sr	9.63 h	$\text{C}(\beta^-)$	15.0(1.7)	^{119m}Te	4.7 d	$\text{I}(\beta^+, \epsilon)$	3.7(5)
^{92}Sr	2.71 h	$\text{C}(\beta^-)$	11.8 (17)	^{121}Te	16.78 d	$\text{C}(\beta^+, \epsilon)$	5.3(10)
^{93}Sr	7.42 m	$\text{C}(\beta^-)$	10.4(22)	^{131m}Te	30 h	$\text{I}(\beta^-)$	6.5(11)
^{84m}Y	39.5 m	$\text{I}(\beta^+, \epsilon)$	3.1 (9)	^{132}Te	3.20 d	$\text{C}(\beta^-)$	6.7(12)
^{87}Y	3.35 d	$\text{C}(\beta^+, \epsilon)$	4.4(7)	^{124}I	4.18 d	$\text{I}(\beta^+, \epsilon)$	10.6(19)
^{88}Y	106.65 d	$\text{C}(\beta^+, \epsilon)$	6.2(10)	^{126}I	13.11 d	$\text{I}(\beta^+/-)$	6.8(18)
^{91m}Y	49.71 m	$\text{C}(\beta^-)$	14(4)	^{130}I	12.36 h	$\text{I}(\beta^-)$	10.0(19)
^{95}Y	10.3 m	$\text{C}(\beta^-)$	17(4)	^{131}I	8.02 d	$\text{C}(\beta^-)$	14.1(23)
^{89}Zr	3.27 d	$\text{C}(\beta^+, \epsilon)$	3.8(7)	^{132}I	2.30 h	$\text{I}(\beta^-)$	8.3(12)
^{95}Zr	64.02 d	$\text{C}(\beta^-)$	36(5)	^{133}I	20.8 h	$\text{C}(\beta^-)$	9.3(14)
^{97}Zr	16.91 h	$\text{C}(\beta^-)$	20(4)	^{134}I	52.6 m	$\text{C}(\beta^-)$	4.3(7)
^{92m}Nb	10.15 d	$\text{I}(\beta^+, \epsilon)$	0.6(4)	^{132}Cs	5.48 d	$\text{I}(\beta^+/-)$	6.2(17)
^{95}Nb	34.98 d	$\text{C}(\beta^-)$	17(2)	^{136}Cs	13.16 d	$\text{C}(\beta^-)$	6.6(12)
^{96}Nb	23.35 h	$\text{I}(\beta^-)$	13.6(17)	^{140}Ba	12.75 d	$\text{C}(\beta^-)$	3.6(6)
^{97}Nb	72.1 m	$\text{C}(\beta^-)$	13.3(21)	^{140}La	1.68 d	$\text{I}(\beta^-)$	7.4(12)
^{98m}Nb	51.3 m	$\text{I}(\beta^-)$	13.9(19)	^{135}Ce	17.7 h	$\text{C}(\beta^+, \epsilon)$	17.0(25)
^{99}Mo	2.75 d	$\text{C}(\beta^-)$	44(6)	^{145}Eu	5.93 d	$\text{C}(\beta^+, \epsilon)$	1.65(19)

Table 4: Experimental data for the target ^{241}Am (continued).

Isotope	$T_{1/2}$	Decay mode	σ_{exp} , mb	Isotope	$T_{1/2}$	Decay mode	σ_{exp} , mb
^{96}Tc	4.98 d	$C(\beta^+, \epsilon)$	2.71(28)	^{146}Eu	4.59 d	$C(\beta^+, \epsilon)$	1.16(17)
^{104}Tc	18.3 m	$C(\beta^-)$	22(6)	^{154}Tb	21.5 h	$C(\beta^+, \epsilon)$	13(6)
^{103}Ru	39.26 d	$C(\beta^-)$	63(10)	^{156}Tb	5.35 d	$C(\epsilon)$	1.7(5)
^{105}Ru	4.44 h	$C(\beta^-)$	34(5)	^{198}Au	2.70 d	$C(\beta^-)$	1.33(20)
^{105}Rh	35.36 h	$C(\beta^-)$	77(13)	^{206}Bi	6.24 d	$C(\epsilon)$	1.21(25)
^{106m}Rh	2.17 h	$I(\beta^-)$	15.0(23)	^{240}Am	50.8 h	$I(\epsilon)$	45(5)

In the **Third Chapter** analysis of the experimental data using theoretical model calculations is performed. In the analysis, calculations with the following computer models, based on the Monte-Carlo method were employed : LAHET (with Bertini and ISABEL cascades, Dresner evaporation and Atchison fission (RAL), and also cascade of Cugnon INCL and fission by Schmidt ABLA, and RAL), Dubna cascade-evaporation-fission model CASCADE (by V.S. Barashenkov), cascade-exciton models CEM95 and CEM2k (S.G. Mashnik, LANL), as well as the four combined models, obtained by joining the cascade parts of CEM2k or Los-Alamos version of quark-gluon model LAQGSM (S.G. Mashnik, K.K. Gudima, LANL) with evaporation-fission parts of generalized evaporation model by S. Furihata GEM2 and the binary fission model by R. Charity GEMINI (LAQGSM+GEM2, CEM2k+GEM2, LAQGSM+GEMINI, CEM2k+GEMINI). Calculations using the programs not modelling fission products (CEM95 and CEM2k) were performed only for analysis of the data from the target $^{129}\text{I}+^{127}\text{I}$. For analysis of the cumulative cross sections, respective theoretical cross sections were also recalculated to cumulative ones, based on known decay branching ratios. Calculations using the basic models of LAHET as well as CEM95 were performed by the author, while the other calculations were carried out by their developers (group of V.S. Barashenkov (JINR), group of S.G. Mashnik, R.E. Prael (LANL, USA)).

Qualitative by-isotope comparison of data from the $^{129}\text{I}+^{127}\text{I}$ with calculations using all these models is shown in **Figure 4**. With the purpose of comparison of the experimental and theoretical values a criterion proposed by R. Michel as well as its standard deviation were used :

$$\langle F \rangle = 10 \sqrt{\langle (\log \sigma_{exp} - \log \sigma_{theo})^2 \rangle} \quad \text{and} \quad S(\langle F \rangle) = 10 \sqrt{\left\langle \left(\left| \log \left(\frac{\sigma_{cal}^i}{\sigma_{exp}^i} \right) \right| - \log(\langle F \rangle) \right)^2 \right\rangle}.$$

Table 5: Theoretical model analysis of the residuals measured in the target $^{127}\text{I}+^{129}\text{I}$.

Model	$A = 44 - 128$			$A \geq 95$		
	$N/N_{30\%}/N_{2.0}$	$\langle F \rangle$	$S(\langle F \rangle)$	$N/N_{30\%}/N_{2.0}$	$\langle F \rangle$	$S(\langle F \rangle)$
LAHET Bertini	36/6/22	3.72	3.00	22/6/19	1.67	1.34
LAHET ISABEL	34/5/18	5.18	4.45	22/5/16	1.72	1.37
LAHET INCL+RAL	33/14/21	3.86	3.16	22/14/21	1.42	1.28
LAHET INCL+ABLA	32/9/21	9.32	7.01	22/9/21	1.57	1.34
CASCADE	42/9/15	11.05	5.19	22/9/14	3.32	2.75
CEM95	40/10/20	5.40	3.52	22/9/18	1.78	1.44
CEM2k	33/13/26	2.89	2.74	22/11/20	1.48	1.27
LAQGS+GEM2	33/13/22	3.16	2.68	22/13/21	1.50	1.34
CEM2k+GEM2	35/10/28	5.03	5.04	22/8/20	1.60	1.35
LAQGS+GEMINI	42/19/29	4.28	3.58	22/17/21	1.31	1.21
CEM2k+GEMINI	42/12/27	2.74	2.15	22/9/20	1.46	1.25

Since a strong dependence of comparison results on the product mass number was observed, two mass regions were chosen : 1) all residuals with $A = 44 - 128$ and 2) only nuclei with $A \geq 95$ (see **Table 5**). Out of 74 cross sections measured in this work, 42 were chosen for such comparison [5,6,7,8] as those meeting the physics principles realized in the models. Particularly, if only an isomer state of a nucleus was measured or, on the contrary, only its ground state was measured whereas this nucleus possesses several rather long-lived isomers having significant branching to the ground state, such cross sections were excluded from the comparison. If the cross sections of a nucleus in both its metastable and ground state be experimentally determined independently, their sum was compared with the calculated value. Results of the qualitative by-isotope analysis for the ^{237}Np target are given in **Figure 5**. For the quantitative comparison using the $\langle F \rangle$ criterion, 37 out of 53 experimentally measured cross sections on ^{237}Np were chosen. For the purpose of analysis, the cross sections were divided into two groups: 1) belonging to the fission region $48 \leq A \leq 175$, and 2) all the residuals [7,8] (see **Table 6**). Results of the qualitative by-isotope analysis for the ^{241}Am target are given in **Figure 6**. For the

Table 6: Theoretical model analysis of the residuals measured in the target ^{237}Np .

Модель	$A = 48 - 175$			$A = 48 - 234$		
	$N/N_{30\%}/N_{2.0}$	$\langle F \rangle$	$S(\langle F \rangle)$	$N/N_{30\%}/N_{2.0}$	$\langle F \rangle$	$S(\langle F \rangle)$
LAHET Bertini	32/4/16	3.29	2.30	37/6/20	3.18	2.26
LAHET ISABEL	32/5/16	3.34	2.37	37/5/19	3.18	2.26
LAHET INCL+RAL	32/7/16	3.51	2.49	37/8/19	3.35	2.39
LAHET INCL+ABLA	32/9/14	4.09	2.78	37/9/14	4.52	2.92
CASCADE	27/4/15	9.75	7.40	32/5/16	11.29	7.75
LAQGSM+GEM2	32/1/14	7.28	4.47	37/2/15	7.10	4.29
CEM2k+GEM2	32/5/16	5.80	3.70	37/6/18	5.43	3.47
LAQGSM+GEMINI	32/4/12	4.69	2.64	36/5/13	4.82	2.69
CEM2k+GEMINI	32/3/10	3.57	1.88	36/4/11	3.87	2.05

quantitative comparison using the $\langle F \rangle$ criterion, 45 out of 80 experimentally measured cross sections on ^{237}Np were chosen. For the purpose of analysis, as before, the cross sections were divided into two groups: 1) belonging to the fission region $48 \leq A \leq 175$, and 2) all the residuals [7,8]. The results of analysis are given in **Table 7**.

Table 7: Theoretical model analysis of the residuals measured in the target ^{241}Am .

Модель	$A = 48 - 175$			$A = 48 - 240$		
	$N/N_{30\%}/N_{2.0}$	$\langle F \rangle$	$S(\langle F \rangle)$	$N/N_{30\%}/N_{2.0}$	$\langle F \rangle$	$S(\langle F \rangle)$
LAHET Bertini	44/19/34	2.28	1.99	37/6/20	3.18	2.26
LAHET ISABEL	44/19/34	2.30	2.01	37/5/19	3.18	2.26
LAHET INCL+RAL	44/14/36	2.44	2.15	37/8/19	3.35	2.39
LAHET INCL+ABLA	44/16/35	2.96	2.69	37/9/14	4.52	2.92
CASCADE	40/7/15	6.57	4.15	32/5/16	11.29	7.75
LAQGSM+GEM2	44/21/33	3.38	3.14	37/2/15	7.10	4.29
CEM2k+GEM2	44/21/32	2.76	2.50	37/6/18	5.43	3.47
LAQGSM+GEMINI	44/8/22	3.69	2.53	36/5/13	4.82	2.69
CEM2k+GEMINI	44/7/17	3.18	2.02	36/4/11	3.87	2.05

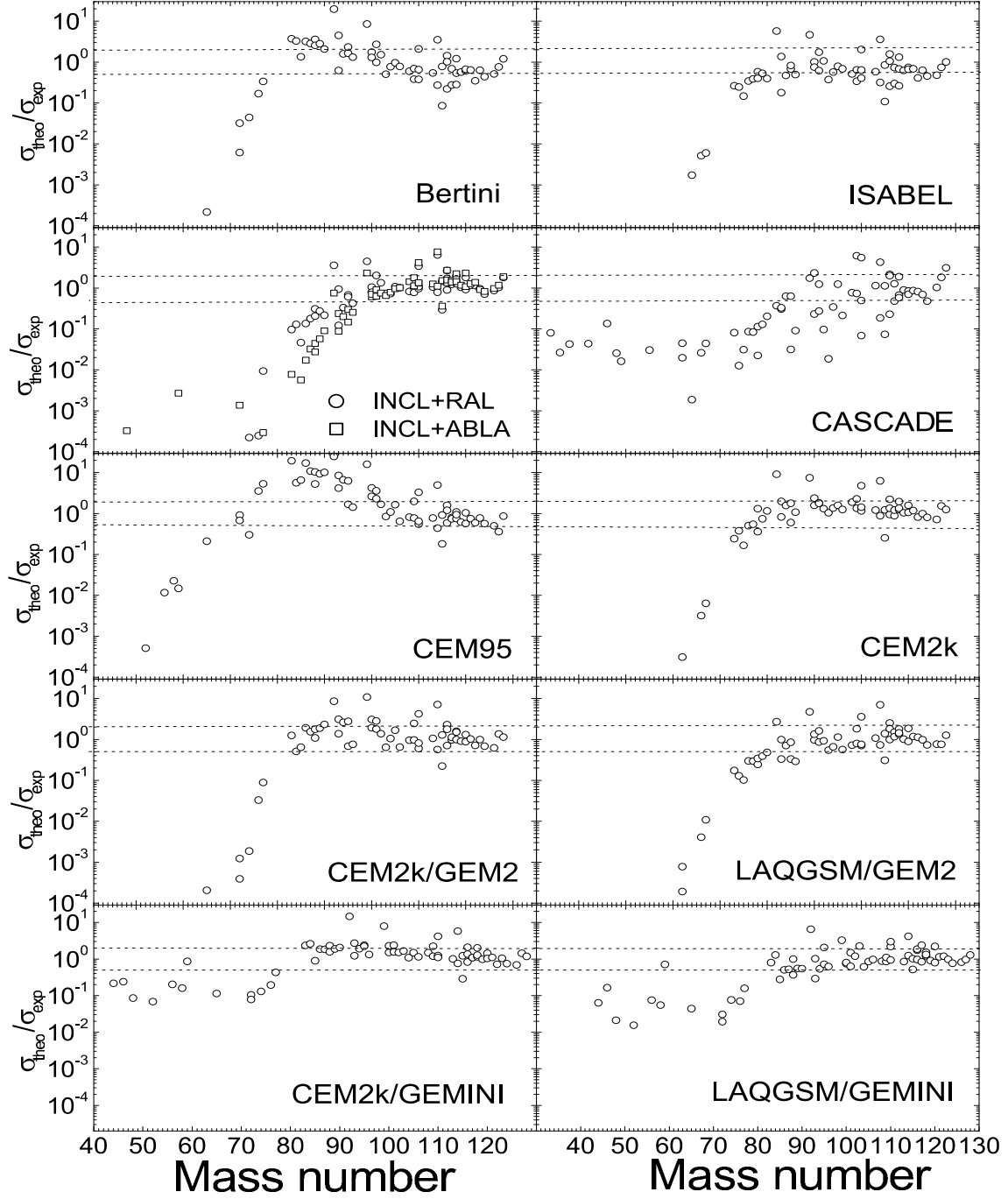


Figure 4: Qualitative theoretical model analysis of the experimental residual formation cross sections in the target 15% ^{127}I + 85% ^{129}I .

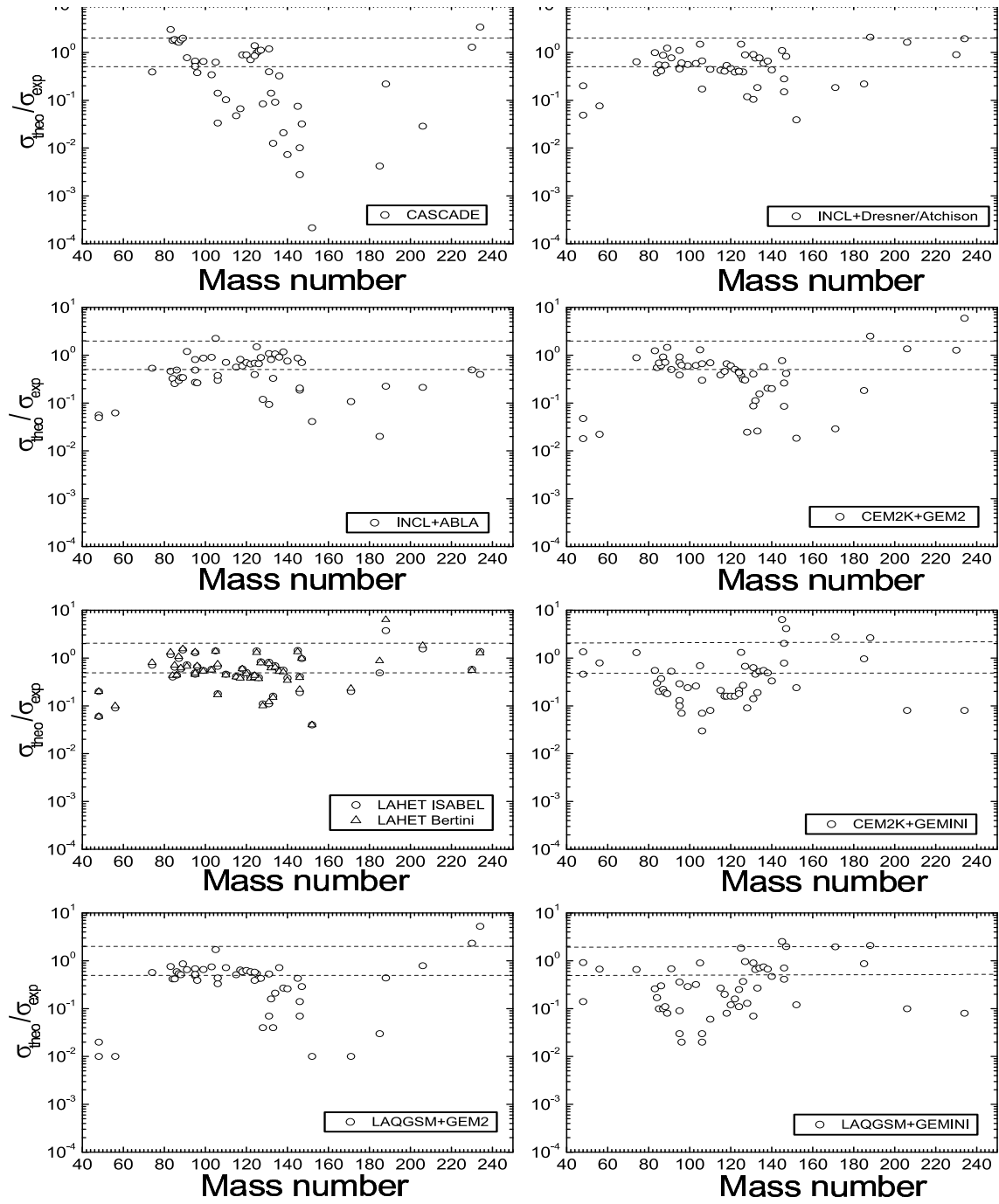


Figure 5: Qualitative theoretical model analysis of the experimental residual formation cross sections in the target ^{237}Np .

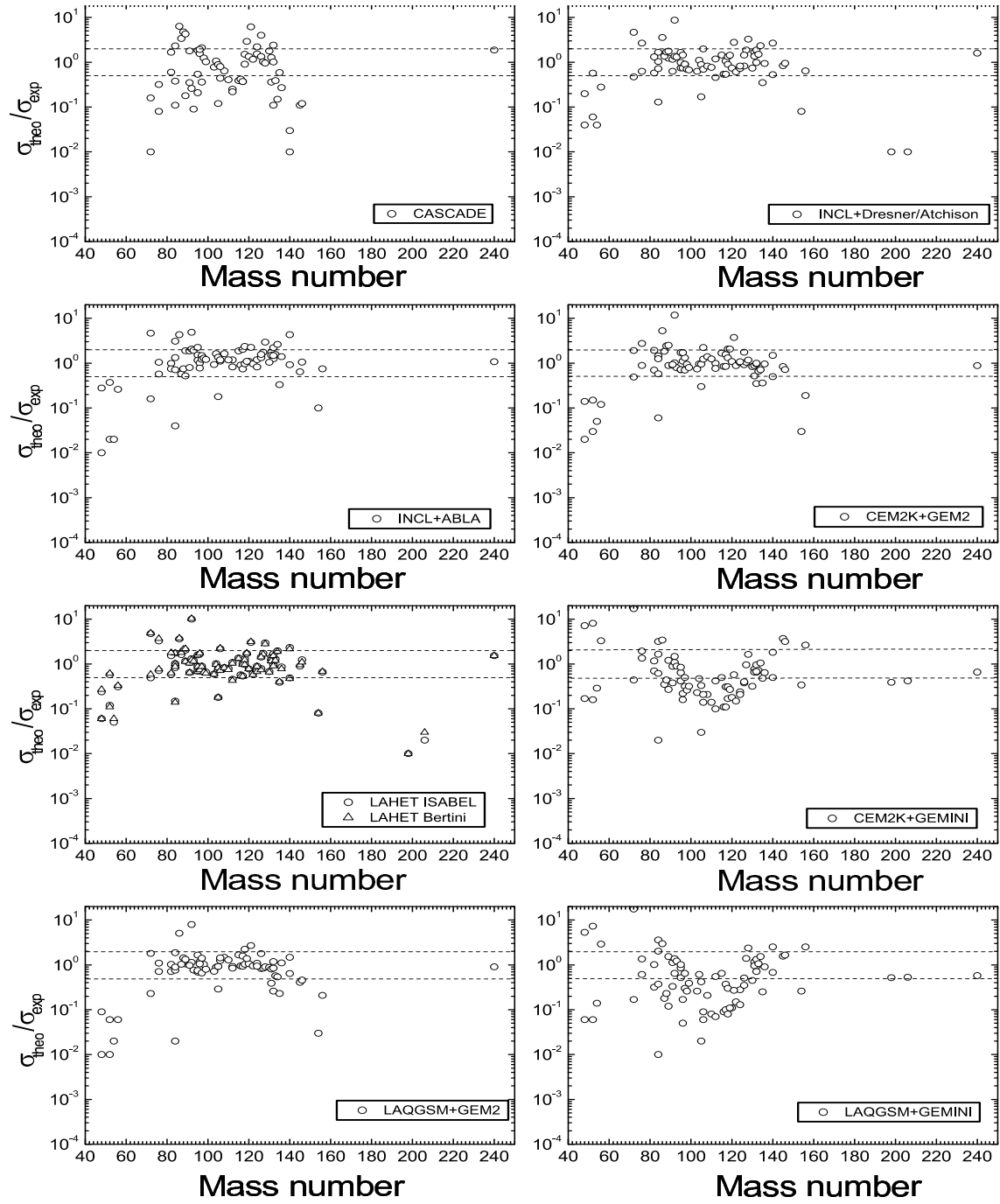


Figure 6: Qualitative theoretical model analysis of the experimental residual formation cross sections in the target ^{241}Am .

In **Conclusion** the main results obtained in the work are summarized:

1. Developed and amended methods of short-lived β -unstable reaction product formation cross section determination employing activation analysis with HPGe spectrometers, taking into account a number of high-precision γ -spectroscopy approaches. Created and implemented a program package.
2. Carried out a high-precision measurement of ^{140}La half-life with the use of a HPGe detector under load change in a wide range, employing a procedure of deadtime underestimation correction. Attained a half-life value in the echelon of accuracy of the recommended values.
3. Developed and demonstrated by the example of $A = 152$ isobar a method for determination of optimal experimental parameters for investigations of individual product nuclides formed with small cross sections in hadron-nuclear interactions, also applicable for study of short-lived β -unstable nuclei situated in complex decay chains.
4. Carried out experiments on determination by γ -spectroscopy formation cross sections of product nuclei in interactions of 660-MeV protons with ^{129}I , ^{237}Np and ^{241}Am targets. Determined 74 residual nuclei in ^{129}I target, 53 residual nuclei in ^{237}Np , and 80 residual nuclei in ^{241}Am . These data were obtained at intermediate energies for the first time.
5. Carried out theoretical model analysis of the product nuclei formation cross sections in ^{129}I , ^{237}Np , and ^{241}Am targets using eleven existing models. Showed that for ^{129}I all the models generally give reasonable agreement with the data for the products with masses higher 95, slightly better results being given by CEM2k+GEMINI and LAQGSM+GEMINI models (LANL, USA). In the case of ^{237}Np and ^{241}Am targets, the best results were shown by Bertini and ISABEL cascade models combined with evaporation-fission model RAL, all of them basic for LAHET and MCNPX (LANL, USA) code systems. High precision of the data measured allowed to demonstrate insufficient for practical applications accuracy of theoretical modelling of the reactions studied.

List of Thesis publications:

- [1] J. Adam, J. Mrázek, J. Frána, A. R. Balabekyan, V. S. Pronskikh, V. G. Kalinnikov, A. N. Priemyshev, “Ionizing Radiation Measurement: Software for Calculating Nuclear Reaction Cross Sections”, *Measurement Techniques* **44**, 93 (2001).
- [2] J. Adam, A.G. Belov, R. Brandt, P. Chaloun, M. Honusek, V.G. Kalinnikov, M.I. Krivopustov, B.A. Kulakov, E.-J. Langrock, M. Ochs, V.S. Pronskikh, A.N. Sosnin, V.I. Stegailov, V.M. Tsoupko-Sitnikov, J.-S. Wan, “ ^{140}La half-life measurement with Ge-detector”, *Nuclear Instruments and Methods in Physics Research* **B187**, 419-426 (2002).
- [3] J. Adam, A. Balabekyan, V.S. Pronskikh, V.G. Kalinnikov, and J. Mrázek, “Determination of the cross section for nuclear reactions in complex nuclear decay chains”, *Applied Radiation and Isotopes* **56**, 607-613 (2002).
- [4] J. Adam, A. Balabekyan, R. Brandt, V.P. Dzhelepov, S.A. Gustov, V.G. Kalinnikov, I.V. Mirokhin, J. Mrázek, R. Odoj, V.S. Pronskikh, O.V. Savchenko, A.N. Sosnin, A.A. Solnyshkin, V.I. Stegailov, V.M. Tsoupko-Sitnikov, “Investigation of the formation of residual nuclei from the radioactive ^{237}Np and ^{241}Am targets in the reaction with 660 MeV protons”, *Physics of Atomic Nuclei* **65**, 763-775 (2002).
- [5] V.S. Pronskikh, J. Adam, A. Balabekyan, V.S. Barashenkov, V.P. Dzhelepov, S.A. Gustov, V.P. Filinova, V.G. Kalinnikov, M.I. Krivopustov, I.V. Mirokhin, A.A. Solnyshkin, V.I. Stegailov, V.M. Tsoupko-Sitnikov, J. Mrázek, R. Brandt, W. Westmeier, R. Odoj, S.G. Mashnik, A.J. Sierk, R.E. Prael, K.K. Gudima, M.I. Baznat, “Study of proton induced reactions in a radioactive ^{129}I target at $E_p=660$ MeV”, *Proceedings of the International Workshop on Nuclear Data for the Transmutation of Nuclear Waste (TRAMU@GSI)*, GSI-Darmstadt, Germany, September 1-5, 2003, ISBN 3-00-012276-1, Eds: A. Kelic and K.-H. Schmidt; LANL Preprint LA-UR-04-2139, pp. 1-6, E-print: nucl-ex/0403056, submitted to *Physical Review C*.
- [6] J. Adam, V.S. Barashenkov, V.P. Dzhelepov, S.A. Gustov, V.P. Filinova, V.G. Kalinnikov, M.I. Krivopustov, I.V. Mirokhin, V.S. Pronskikh, A.A. Sol-

nyshkin, V.I. Stegailov, V.M. Tsoupko-Sitnikov, J. Mrázek, R. Brandt, W. Westmeier, R. Odoj, S.G. Mashnik, R.E. Prael, K.K. Gudima, M.I. Baznat, “Investigation of proton-nuclear reaction product formation in ^{129}I target at 660-MeV proton energy” (in Russian), ECHAYA Letters 4(121), 53-64 (2004).

- [7] J. Adam, A. Balabekyan, R. Brandt, V.S. Barashenkov, V.P. Dzhelepov, V.P. Filinova, S.A. Gustov, V.G. Kalinnikov, M.I. Krivopustov, I.V. Mirokhin, J. Mrázek, R. Odoj, V.S. Pronskikh, O.V. Savchenko, A.N. Sosnin, A.A. Solnyshkin, V.I. Stegailov, V.M. Tsoupko-Sitnikov, “Investigation of the formation of residual nuclei in reactions induced by 660 MeV protons interacting with the radioactive ^{237}Np , ^{241}Am and ^{129}I targets”, Journal of Nuclear Science and Technology, Supplement 2, 272-275 (August 2002).
- [8] S.G. Mashnik, V.S. Pronskikh, J. Adam, A. Balabekyan, V.S. Barashenkov, V.P. Filinova, A.A. Solnyshkin, V.M. Tsoupko-Sitnikov, R. Brandt, R. Odoj, A.J. Sierk, R.E. Prael, K.K. Gudima, M.I. Baznat, “Analysis of the JINR p(660 MeV) + ^{129}I , ^{237}Np , and ^{241}Am measurements with eleven different models”, LANL Preprint LA-UR-04-4929, стр. 1-12, E-print: nucl-th/0407097, Proceedings of the 7th Specialists’ Meeting on Shielding Aspect of Accelerators, Targets and Irradiated Facilities, SATIF-7, Sacavem (Lisbon), Portugal, May 17-18, 2004.